Вестник РУДН. Серия: Инженерные исследования
RUDN Journal of Engineering Researches
2021;22(1):84–99
journals.rudn.ru/engineering-researches

DOI: 10.22363/2312-8143-2021-22-1-84-99
УДК 69.002.5

Research article / Научная статья

Pseudospheric shells in the construction

Mathieu Gil-oulbé*, Ipel Junior A. Ndomilep, Prosper Ngandu

Peoples' Friendship University of Russia (RUDN University),
6 Miklukho-Maklaya St, Moscow, 117198, Russian Federation
*E-mail: gil-oulbem@hotmail.com

Article history
Received: October 29, 2020
Revised: January 09, 2021
Accepted: February 20, 2021

Keywords: pseudosphere, Beltramy surface, tractix, bending calculation theory, temporal calculation theory, pseudosphere resistance

Abstract. The architects working with the shell use well-established geometry forms, which make up about 5—10 % of the number of known surfaces, in their projects. However, there is such a well-known surface of rotation, which from the 19th century to the present is very popular among mathematicians-geometers, but it is practically unknown to architects and designers, there are no examples of its use in the construction industry. This is a pseudosphere surface. For a pseudospherical surface with a pseudosphere rib radius, the Gaussian curvature at all points equals the constant negative number. The pseudosphere, or the surface of the Beltram, is generated by the rotation of the tracersis, evolvent of the chain line. The article provides an overview of known methods of calculation of pseudospherical shells and explores the strain-stress state of thin shells of revolution with close geometry parameters to identify optimal forms. As noted earlier, no examples of the use of the surface of the pseudosphere in the construction industry have been found in the scientific and technical literature. Only Kenneth Becher presented examples of pseudospheres implemented in nature: a gypsum model of the pseudosphere made by V. Martin Schilling at the end of the 19th century.

For citation
Gil-oulbé M, Ndomilep IJA, Ngandu P. Pseudospheric shells in the construction. *RUDN Journal of Engineering Researches*. 2021;22(1):84–99. http://dx.doi.org/10.22363/2312-8143-2021-22-1-84-99

Псевдосферические оболочки в строительстве

М. Жиль-улбе*, И.Дж.А. Ндомилеп, П. Нганду

Российский университет дружбы народов,
Российская Федерация, 117198, Москва, ул. Миклухо-Маклая, д. 6
*E-mail: gil-oulbem@hotmail.com

История статьи
Поступила в редакцию: 29 октября 2020 г.
Доработана: 09 января 2021 г.
Принята к публикации: 20 февраля 2021 г.

Аннотация. Архитекторы, работающие с оболочкой, используют в своих проектах хорошо зарекомендовавшие себя геометрические формы, которые составляют около 5-10% от числа известных поверхностей. Однако есть такая известная поверхность вращения, которая с XIX в. по настоящее время пользуется большой популярностью среди математиков-геометров, но практически неизвестна архитекторам и дизайнерам, нет примеров ее применения в строительной отрасли. Это поверхность псевдосферы. Для псевдосферической поверхности гауссова кривизна во всех точках равна постоянному отрицательному числу. Псевдосфера, или поверхность Бельтрами, образуется вращением трактрисы. Псевдосфера, или поверхность Бельтрами, образуется вращением трассерсиса, эволюционирующего из цепной линии. В статье дается обзор известных методов расчета псевдосферических оболочек и исследуется напряженно-деформированное состояние тонких оболочек вращения с близкими геометрическими параметрами для определения оптимальных форм. Как отмечалось ранее, в научно-технической литературе не найдены примеры применения поверхности псевдосферы в строительной отрасли. Только Кеннет Бехер представил примеры псевдосфер, реализованных в природе: гипсовая модель псевдосферы, сделанная В. Мартином Шиллингом в конце XIX века.

Ключевые слова: псевдосфера, поверхность Бельтрами, трактриса, теория расчета на изгиб, теория временных расчетов, прочность псевдосферических оболочек

Для цитирования

Gil-oulbé M., Ndomilep I.J.A., Ngandu P. Pseudospheric shells in the construction // Вестник Российского университета дружбы народов. Серия: Инженерные исследования. 2021. Т. 22. № 1. С. 84–99. http://dx.doi.org/10.22363/2312-8143-2021-22-1-84-99

Introduction

The most famous modern architects can be divided into three groups. One group seeks to build [1] high — rise facilities while saving expensive land, especially in urban areas. These architects believe that big — flying structures are necessary only if they are functionally needed. In some cases, large — flying structures have even been demolished to make room for high — rise buildings (Moscow, Minsk, Belarus) or for a more profitable building (The King Dome, Seattle, USA). Another group believes that it is more comfortable for a person to be closer to the ground [2]. They join the former President of the International Shell Association (1966), Prof. A.M. Haas: “The people who build the shells are advanced people; They are united by the desire for new forms, new ways of solving problems” [3] and, by applying scientific approaches to analyse and design large — span structures, they have achieved outstanding success [4]. The third group believes that using traditional constructions (walls, columns, flat overlays) and rectangular shapes, it is also possible to get good results. They focus on low — cost model designs, shapes and high — end materials.

The architects working with the shell use well established geometry forms, which make up about 5—10 % of the number of known surfaces, in their projects. These are paraboloids of revolution [5], umbrella — shaped, apple — shaped, cyclic, propeller, cylindrical shell [6], conic shell [7], mid — surface shell in the form of conoid and cylindroid [8], elliptical paraboloid [9], single — striped hyperboloid [10] and some others [11]. In each particular case, architects and design engineers chose the most optimal shape of the shell based on functional necessity, strength, aesthetics, etc.

However, there is such a well — known surface of revolution, which from the 19th century to the present is the focus of mathematicians — geometers [12—18], but it is almost unknown to architects and designers, there are no examples of its application in the construction industry. This is a pseudo — sphere surface.

1. Characteristics and methods of setting the pseudosphere

For pseudosphere surface (Figure 1, Figure 2) radius a Gaussian curvature $K = k_1k_2$ at all points equals a constant negative number $K = -1 / a^2$.

Pseudosphere, or the surface of the Beltram, is formed by rotation of tracersis, chain line involutes $r = ach(z/a)$, relative to the z-axis.

The equation of the tractix is

$$x = a \sin u,\ z = a\left[\cos u + \ln \operatorname{tg}(u/2)\right],\ 0 < u < \pi ,$$

where u – involute of a catenary line, the angle between the y-axis and tangent to tractices.
The tractix equation can also be written as

$$z = a\ln\frac{a \pm \sqrt{a^2 - r^2}}{r} \mp \sqrt{a^2 - r^2},$$

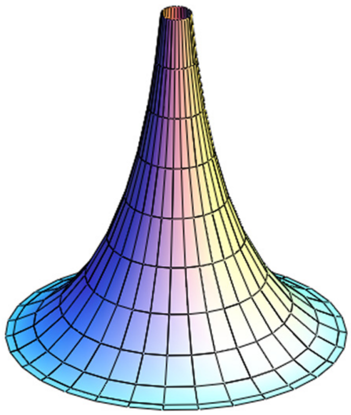

Figure 1. One pseudosphere cavity

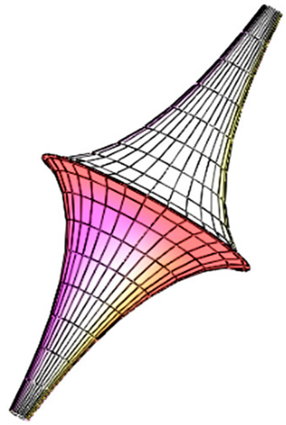

Figure 2. Pseudo-space with two canvas

where the upper signs refer to the positive branch $z > 0$, lower to negative $z < 0$ (Figure 2). The length of the segment tangent to the tractor from the point of contact to the point of intersection with the z-axis – constant and equal to $a > 0$. The section line of the pseudosphere by the xOy plane (edge of the pseudosphere) – is a circle of radius a, for all other parallels $r < a$. The volume of one floor of the pseudosphere: $V = \pi a^3/3$.

Three forms of pseudosphere definition are known using parametric equations [19]. For further application, let us use the following parametric form of pseudosphere surface setting:

$$x = x(r,\beta) = r\cos\beta, \quad y = y(r,\beta) = r\sin\beta,$$

$$z = z(r) = a\ln\left[\left(a + \sqrt{a^2 - r^2}\right)/r\right] - \sqrt{a^2 - r^2},$$

where r is the distance from the rotation axis to the corresponding pseudosphere point ($r < a$), circle $r = r_{max} = a$ – is the pseudosphere edge. Area between parallels $r = a$ and $r = r_o$:

$$S = 2\pi a(a - r_o).$$

In this case, the coefficients of the basic quadratic forms of the surface and its main curvatures are:

$$A = \frac{a}{r}, \; F = 0, \; B = r, \; L = \frac{a}{r\sqrt{a^2 - r^2}},$$

$$M = 0, \; N = -\frac{r\sqrt{a^2 - r^2}}{a}, \; k_1 = \frac{r}{a\sqrt{a^2 - r^2}},$$

$$k_2 = -\frac{\sqrt{a^2 - r^2}}{ar}.$$

Therefore, the pseudosphere is defined in curved orthogonal contiguous coordinates. r, β, i.e., in the lines of the main curves. “Appeal in the middle of the XIX century. Geometers to pseudospheric surfaces, surfaces of constant negative curvature $K = -1/a^2$, it was an important step in the development of mathematics. Pseudospherical surfaces were of great importance for the visual interpretation of non-Euclidean hyperbolic geometry discovered by N.I. Lobachevsky. The subsequent development of mathematics revealed a close connection of pseudospherical surfaces with network theory, soliton theory, attractors, nonlinear equations of mathematical physics, Becklund transformations, etc.” [12].

2. Overview of pseudosphere shell analyses

The membrane theory of analysing pseudospherical shells was realized by V.G. Rekach [20] for the case of a homogeneous problem. The solution was made in the form of a trigonometric series. He also determined the tangential forces in the pseudospherical shell of constant thickness from its self-weight, supported hinged-movably in the normal direction in a parallel circle $r = 0{,}5a$.

The bending theory of analysis of pseudospherical shells in a linear formulation subject to surface symmetric and inversely symmetric loads was considered in the work of D. Werner [21]. The solution was made in analytical form. A numerical example of the analysis is presented in tabular form. To simplify the analysis, the Poisson's ratio was assumed to be zero.

The first attempt to make an overview of all the works devoted to pseudospherical surfaces and shells was made in 1998 in the article [22]. In it, in addition to the investigations of E. Beltrami, V.G. Rekach [20], D. Werner [21], the results obtained by B. Bhattacharya [23] and A.P. Filin [24] are described. A.P. Filin gave formulas for analysing the deformation parameters, the equation of continuity of deformations and the equation of equilibrium of the element of the pseudospherical shell given in the curvature lines. Krawczyk J. [32] considered infinitesimal deformations of thin elastic shells of constant thickness.

A.A. Kalashnikov [30] determined the normal forces in the pseudospherical shell subject to its self-weight by the membrane theory. He then, using the SCAD FEM program, analysed the same shell also subject to its self-weight. Comparison of the results showed a large difference in the values of the ring normal forces on the support. Bending moments are mainly concentrated near the bottom support by the type of edge effect.

In recent years, appeared the first studies on stability of pseudospherical shells. Mikheev A.V. [25], Jasion P., Magnucki K. [26; 27] are working on this issue.

3. Stress-strain state of shells of revolution with close geometric parameters

There are a number of works, for example [29], where some criteria are put forward for assessing the optimality of the selected design solution. V.V. Novozhilov [29] suggested using the results of their analysis according to the membrane theory for an approximate estimate of the optimality of the chosen form of the thin-walled shell of revolution. Shells with similar geometric parameters (boom lifting and diameter of the shell at the base) were chosen for the analysis.

Let's follow his example. Figure 3 shows five types of shells of revolution. The pseudospherical (Figure 3, a), conical shell (Figure 3, b), a shell with a median surface of revolution of the hyperbola $z = \frac{b}{x}$ around the z-axis (Figure 3, c), a shell with the median surface of revolution of the asteroid (Figure 3, d) and in the form of a one-sheeted hyperboloid of revolution (Figure 3, e).

All these surfaces are defined by parametric equations: $x = x(r, \beta) = r\cos\beta$, $y = y(r, \beta) = r\sin\beta$, $z = z(r)$, where for the pseudosphere (Figure 3, a):

$$z = z(r) = a\ln\frac{a + \sqrt{a^2 - r^2}}{r} - \sqrt{a^2 - r^2},$$

for the cone (Figure 3, b):

$$z = z(r) = -\frac{rH}{r_1 - r_2},$$

for the surface of rotation of the hyperbola $z = b/x$ around the axis Oz (Figure 3):

$$z = z(r) = \frac{Hr_1r_2}{(r_1 - r_2)r}.$$

For the surface of the rotation of the asteroid (Figure 3, g):

$$z = z(r) = (b^{\frac{2}{3}} - r^{\frac{2}{3}})^{3/2},$$

the parameter b must be found from the equality:

$$H = (b^{2/3} - r_2^{2/3})^{3/2} - (b^{2/3} - r_1^{2/3})^{3/2},$$

for a single-cavity hyperboloid of revolution (Figure 3, d):

$$z = z(r) = \frac{-H\sqrt{r^2 - b^2}}{(\sqrt{r_1^2 - b^2} - \sqrt{r_2^2 - b^2})}.$$

where parameter b can take any value, but $b < r_2$.

All unspecified geometric parameters are shown in Figure 3. In the same figure, the meridians of the pseudosphere are shown by a solid line, and the meridians of the remaining surfaces of revolution are shown by a thin line with dots.

Shell thickness $h = 0.05$ *cm*, self-weight type surface load $q = 100$ *kg / m*^{2}, the radius of the base is $r_1 = 4$ *m*, the radius of the hole in the apex is $r_2 = 2$ *m*, the boom of lifting $H = 5.15$ *m* is the same for all shells, $r_2 \le r \le r_1,\ 0 \le \beta \le 2\pi$.

Under axisymmetric loading of the shells of revolution, the surface distributed load in the direction of the curvilinear coordinate β is zero ($Y = 0$), normal forces (N_r, N_β), shearing forces (Q_r), bending moments (M_r, M_β), deformations (ε_r, ε_β, κ_r, κ_β) and displacements

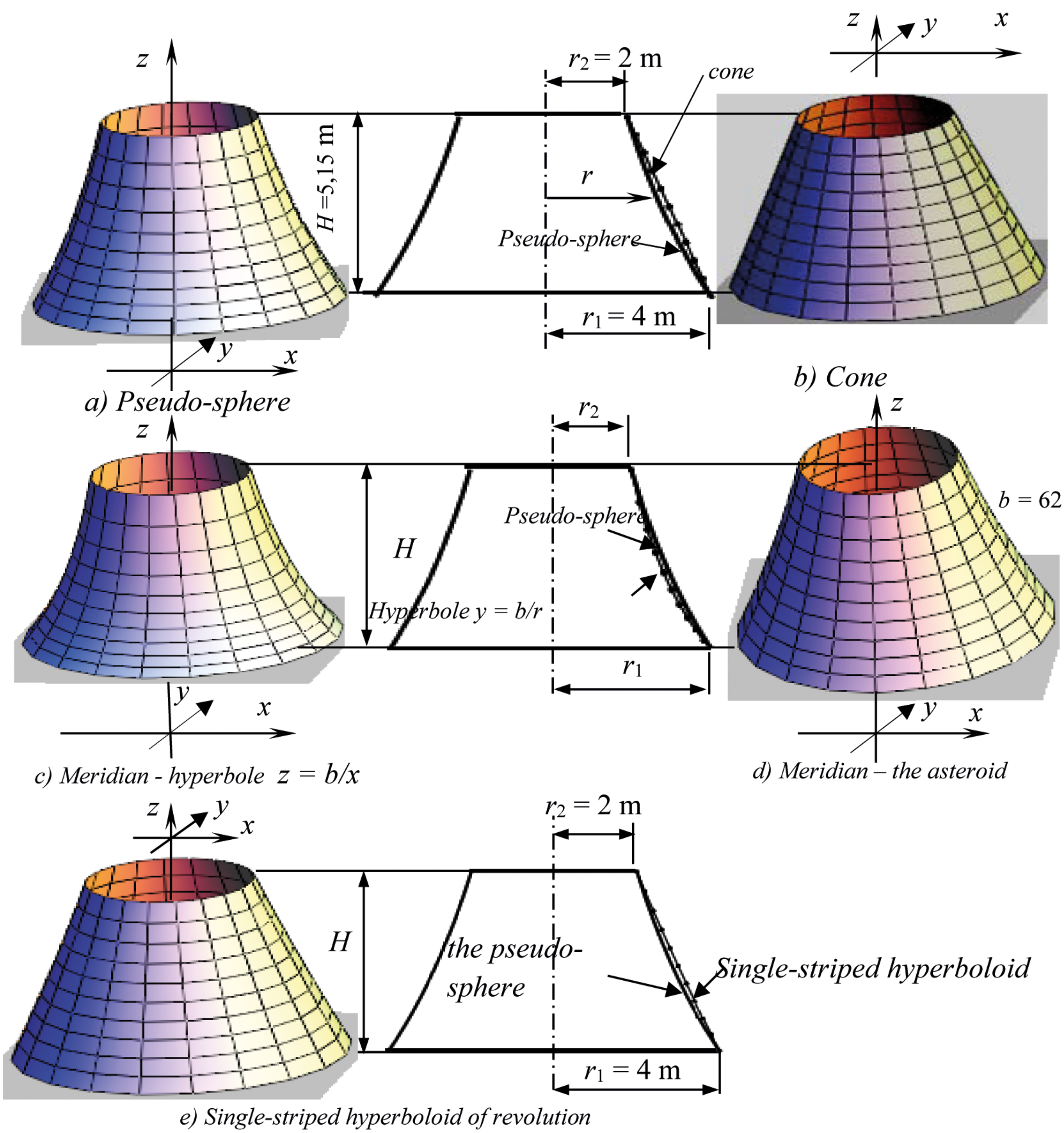

Figure 3. Five types of rotation surfaces

($W = u_Z$, u_r) are independent of the longitude angle β, and, in addition,

$$S = Q_\beta = M_{r\beta} = 0,\ \ u_\beta = \varepsilon_{r\beta} = \kappa_{r\beta} = 0.$$

Figures 4—28 present the analysis results of the shells of revolution considered subject to self-weight by the finite elements method with a pivotally fixed support of the lower edge ($r = r_1$) and the free upper edge ($r = r_2$). Accepted $E = 3.5{\cdot}10^4$ MPa, Poisson's ratio ν = 0.1.

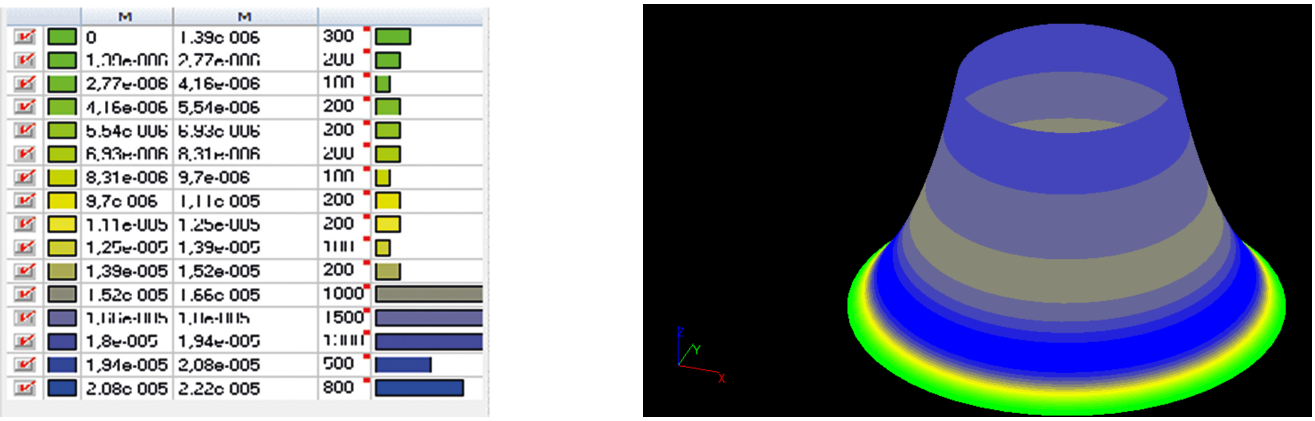

		M	M		
		0	1,39e-006	300	
		1,39e-006	2,77e-006	200	
		2,77e-006	4,16e-006	100	
		4,16e-006	5,54e-006	200	
		5,54e-006	6,93e-006	200	
		6,93e-006	8,31e-006	200	
		8,31e-006	9,7e-006	100	
		9,7e-006	1,11e-005	200	
		1,11e-005	1,25e-005	200	
		1,25e-005	1,39e-005	[illegible]	
		1,39e-005	1,52e-005	200	
		1,52e-005	1,66e-005	1000	
		[illegible]	[illegible]	1500	
		1,8e-005	1,94e-005	[illegible]	
		1,94e-005	2,08e-005	500	
		2,08e-005	2,22e-005	800	

Figure 4. The overall displacement of Pseudosphere

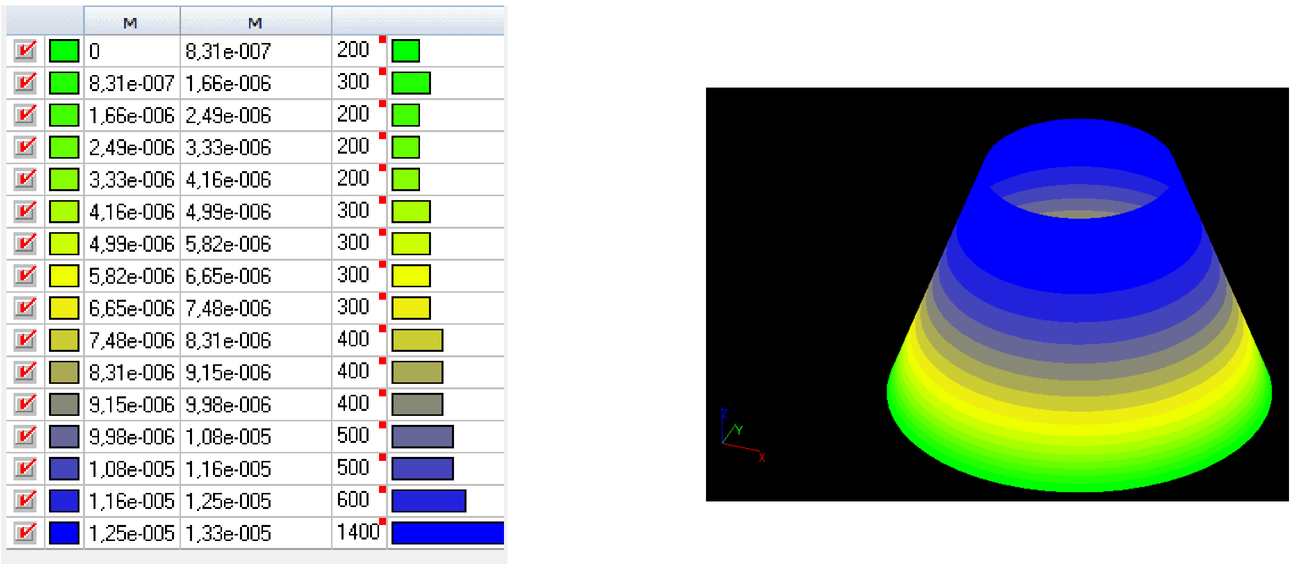

		M	M		
		0	8,31e-007	200	
		8,31e-007	1,66e-006	300	
		1,66e-006	2,49e-006	200	
		2,49e-006	3,33e-006	200	
		3,33e-006	4,16e-006	200	
		4,16e-006	4,99e-006	300	
		4,99e-006	5,82e-006	300	
		5,82e-006	6,65e-006	300	
		6,65e-006	7,48e-006	300	
		7,48e-006	8,31e-006	400	
		8,31e-006	9,15e-006	400	
		9,15e-006	9,98e-006	400	
		9,98e-006	1,08e-005	500	
		1,08e-005	1,16e-005	500	
		1,16e-005	1,25e-005	600	
		1,25e-005	1,33e-005	1400	

Figure 5. The overall displacement of Cone

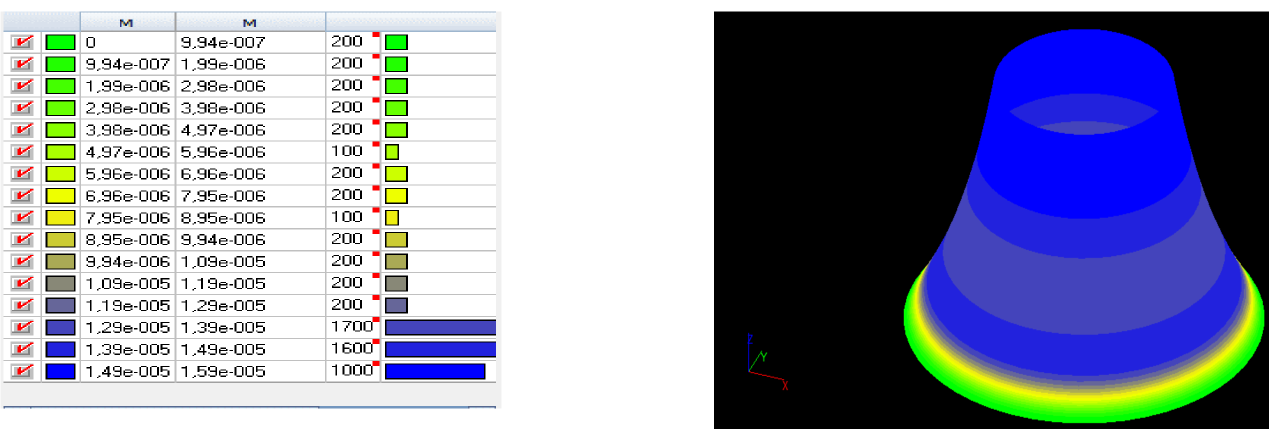

		M	M		
		0	9,94e-007	200	
		9,94e-007	1,99e-006	200	
		1,99e-006	2,98e-006	200	
		2,98e-006	3,98e-006	200	
		3,98e-006	4,97e-006	200	
		4,97e-006	5,96e-006	100	
		5,96e-006	6,96e-006	200	
		6,96e-006	7,95e-006	200	
		7,95e-006	8,95e-006	100	
		8,95e-006	9,94e-006	200	
		9,94e-006	1,09e-005	200	
		1,09e-005	1,19e-005	200	
		1,19e-005	1,29e-005	200	
		1,29e-005	1,39e-005	1700	
		1,39e-005	1,49e-005	1600	
		1,49e-005	1,59e-005	1000	

Figure 6. The overall displacement of Meridian – Hyperbole

0	8,37e-007	200
8,37e-007	1,67e-006	200
1,67e-006	2,51e-006	300
2,51e-006	3,35e-006	200
3,35e-006	4,19e-006	200
4,19e-006	5,02e-006	200
5,02e-006	5,86e-006	300
5,86e-006	6,7e-006	200
6,7e-006	7,53e-006	400
7,53e-006	8,37e-006	400
8,37e-006	9,21e-006	500
9,21e-006	1,e-005	400
1,e-005	1,09e-005	500
1,09e-005	1,17e-005	500
1,17e-005	1,26e-005	600
1,26e-005	1,34e-005	1400

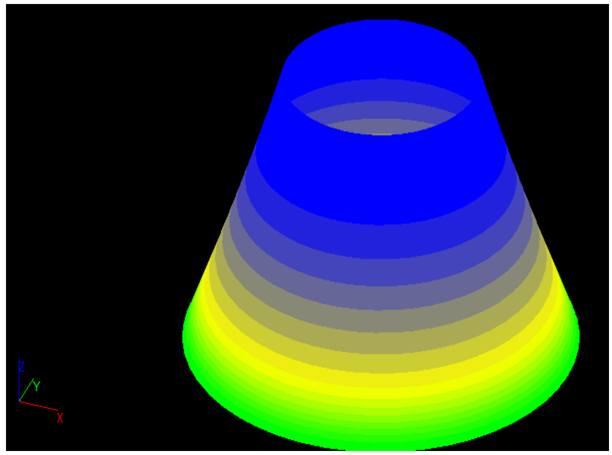

Figure 7. The overall displacement of Meridian – Asteroid

м	м	
0	6,94e-008	200
6,94e-008	1,39e-007	300
1,39e-007	2,08e-007	200
2,08e-007	2,77e-007	200
2,77e-007	3,47e-007	200
3,47e-007	4,16e-007	200
4,16e-007	4,86e-007	300
4,86e-007	5,55e-007	300
5,55e-007	6,24e-007	300
6,24e-007	6,94e-007	400
6,94e-007	7,63e-007	500
7,63e-007	8,32e-007	400
8,32e-007	9,02e-007	500
9,02e-007	9,71e-007	500
9,71e-007	1,04e-006	600
1,04e-006	1,11e-006	1400

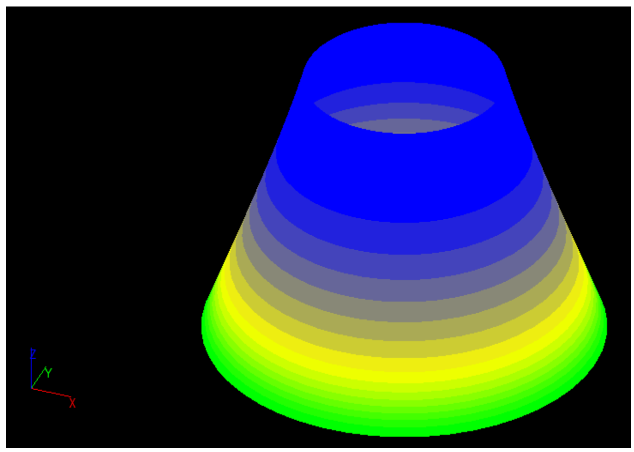

Figure 8. The overall displacement of Single-cavity hyperboloid of revolution

N_x кН/м²	кН/м²	
-147,74	-138,71	350
-138,71	-129,68	700
-129,68	-120,64	1500
-120,64	-111,61	1300
-111,61	-102,58	1100
-102,58	-93,55	950
-93,55	-84,52	950
-84,52	-75,48	1000
-75,48	-66,45	850
-66,45	-57,42	900
-57,42	-48,39	900
-48,39	-39,36	850
-39,36	-30,32	750
-30,32	-21,29	500
-21,29	-12,26	400
-12,26	-3,23	200

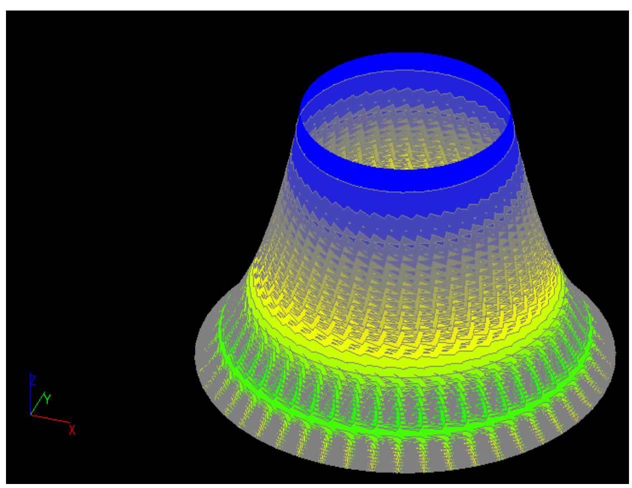

Figure 9. The Normal effort of Pseudosphere about the x-axis

N_x		
кН/м²	кН/м²	
-128,69	-120,76	200
-120,76	-112,82	400
-112,82	-104,88	600
-104,88	-96,95	750
-96,95	-89,01	950
-89,01	-81,08	1150
-81,08	-73,14	1900
-73,14	-65,21	1750
-65,21	-57,27	1850
-57,27	-49,34	2000
-49,34	-41,4	2150
-41,4	-33,47	1650
-33,47	-25,53	1000
-25,53	-17,6	650
-17,6	-9,66	450
-9,66	-1,73	150

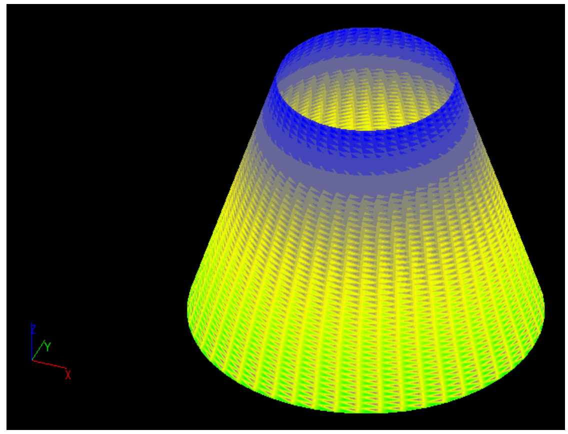

Figure 10. The Normal effort of Cone about the x-axis

N_x		
кН/м²	кН/м²	
-132,61	-124,52	450
-124,52	-116,43	750
-116,43	-108,33	1350
-108,33	-100,24	1500
-100,24	-92,15	1300
-92,15	-84,06	1250
-84,06	-75,96	1300
-75,96	-67,87	1150
-67,87	-59,78	1050
-59,78	-51,69	1050
-51,69	-43,59	950
-43,59	-35,5	850
-35,5	-27,41	700
-27,41	-19,32	400
-19,32	-11,22	300
-11,22	-3,13	200

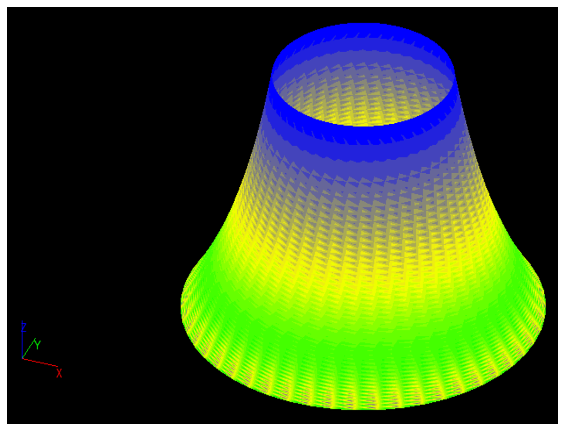

Figure 11. The Normal effort of Meridian – Hyperbole about the x-axis

N_x		
кН/м²	кН/м²	
-128,89	-120,96	250
-120,96	-113,03	450
-113,03	-105,09	650
-105,09	-97,16	800
-97,16	-89,22	1050
-89,22	-81,29	1200
-81,29	-73,36	2150
-73,36	-65,42	1750
-65,42	-57,49	1850
-57,49	-49,55	2050
-49,55	-41,62	1800
-41,62	-33,69	1250
-33,69	-25,75	850
-25,75	-17,82	600
-17,82	-9,88	450
-9,88	-1,95	150

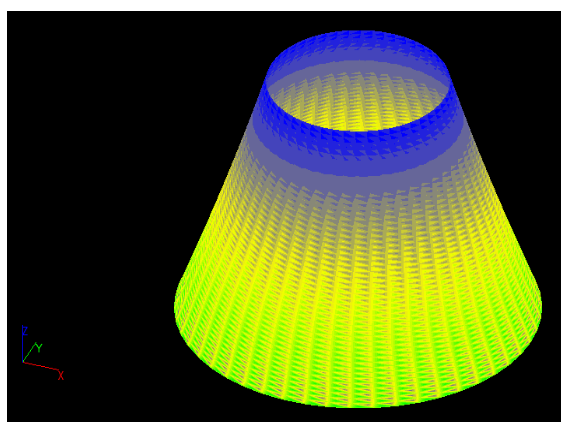

Figure 12. The Normal effort of Meridian – Asteroid about the x-axis

N_x		
кН/м^2	кН/м^2	
-10,7	-10,04	250
-10,04	-9,38	450
-9,38	-8,73	650
-8,73	-8,07	800
-8,07	-7,41	1050
-7,41	-6,75	1200
-6,75	-6,1	2100
-6,1	-5,44	1850
-5,44	-4,78	1950
-4,78	-4,12	2000
-4,12	-3,47	2050
-3,47	-2,81	1350
-2,81	-2,15	750
-2,15	-1,49	550
-1,49	-0,83	450
-0,83	-0,18	200

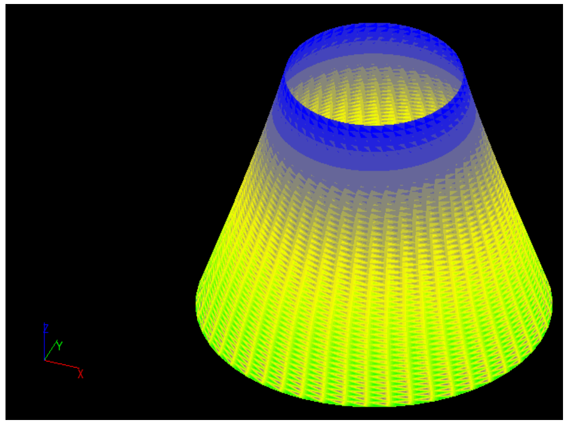

Figure 13. The Normal effort of Single-cavity hyperboloid of revolution about the x-axis

N_y		
кН/м^2	кН/м^2	
-148,5	-139,61	300
-139,61	-130,71	1250
-130,71	-121,82	1500
-121,82	-112,92	1350
-112,92	-104,02	1150
-104,02	-95,13	1050
-95,13	-86,23	900
-86,23	-77,33	950
-77,33	-68,44	850
-68,44	-59,54	850
-59,54	-50,64	850
-50,64	-41,75	850
-41,75	-32,85	800
-32,85	-23,96	700
-23,96	-15,06	500
-15,06	-6,16	300

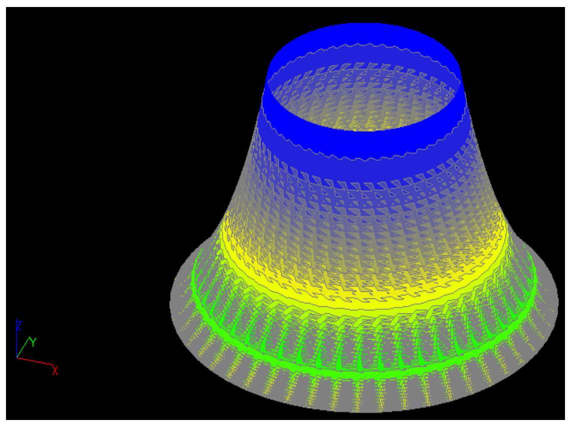

Figure 14. The Normal effort of Pseudosphere about the y-axis

N_y		
кН/м^2	кН/м^2	
-123,74	-116,34	250
-116,34	-108,93	400
-108,93	-101,52	600
-101,52	-94,11	750
-94,11	-86,7	900
-86,7	-79,3	1050
-79,3	-71,89	1750
-71,89	-64,48	1750
-64,48	-57,07	1850
-57,07	-49,66	1950
-49,66	-42,26	2100
-42,26	-34,85	2250
-34,85	-27,44	1550
-27,44	-20,03	900
-20,03	-12,62	550
-12,62	-5,22	200

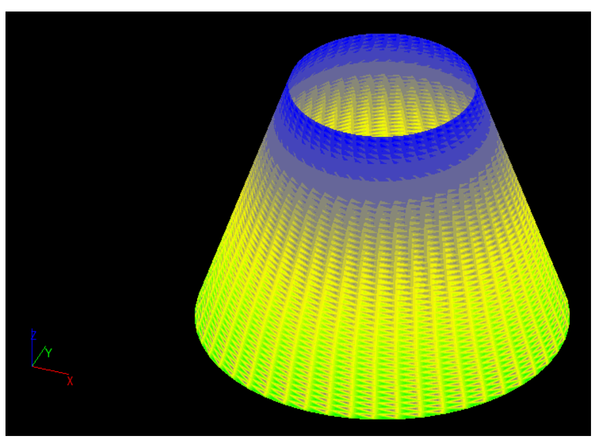

Figure 15. The Normal effort of Cone about the y-axis

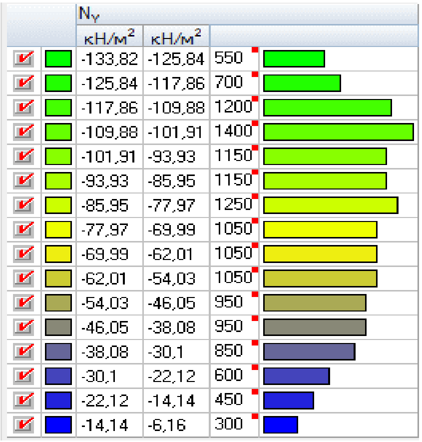

N_Y		
кН/м²	кН/м²	
-133,82	-125,84	550
-125,84	-117,86	700
-117,86	-109,88	1200
-109,88	-101,91	1400
-101,91	-93,93	1150
-93,93	-85,95	1150
-85,95	-77,97	1250
-77,97	-69,99	1050
-69,99	-62,01	1050
-62,01	-54,03	1050
-54,03	-46,05	950
-46,05	-38,08	950
-38,08	-30,1	850
-30,1	-22,12	600
-22,12	-14,14	450
-14,14	-6,16	300

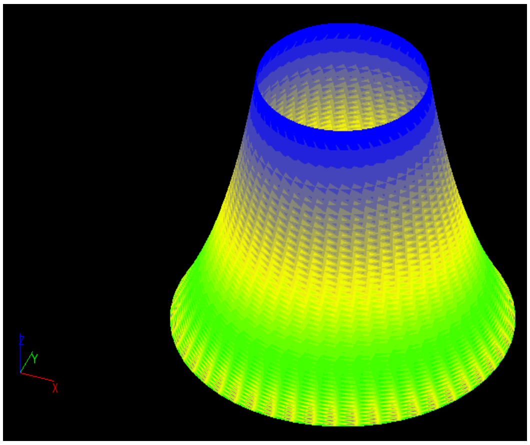

Figure 16. The Normal effort of Meridian – Hyperbole about the x-axis

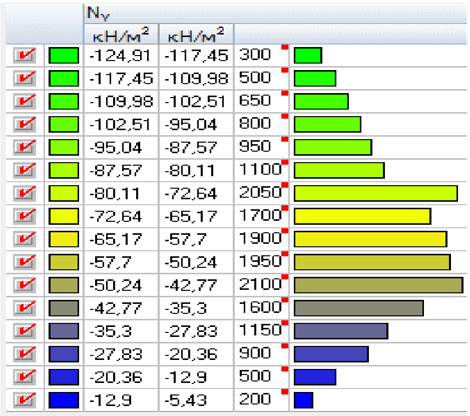

N_Y		
кН/м²	кН/м²	
-124,91	-117,45	300
-117,45	-109,98	500
-109,98	-102,51	650
-102,51	-95,04	800
-95,04	-87,57	950
-87,57	-80,11	1100
-80,11	-72,64	2050
-72,64	-65,17	1700
-65,17	-57,7	1900
-57,7	-50,24	1950
-50,24	-42,77	2100
-42,77	-35,3	1600
-35,3	-27,83	1150
-27,83	-20,36	900
-20,36	-12,9	500
-12,9	-5,43	200

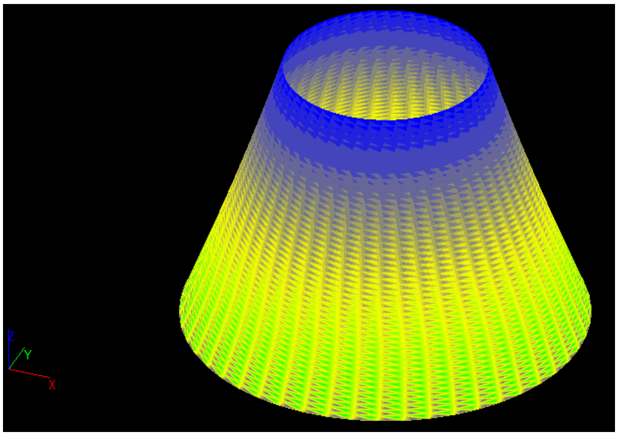

Figure 17. The Normal effort of Meridian – Asteroid about the y-axis

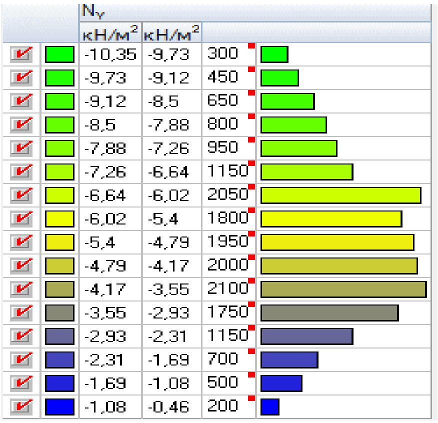

N_Y		
кН/м²	кН/м²	
-10,35	-9,73	300
-9,73	-9,12	450
-9,12	-8,5	650
-8,5	-7,88	800
-7,88	-7,26	950
-7,26	-6,64	1150
-6,64	-6,02	2050
-6,02	-5,4	1800
-5,4	-4,79	1950
-4,79	-4,17	2000
-4,17	-3,55	2100
-3,55	-2,93	1750
-2,93	-2,31	1150
-2,31	-1,69	700
-1,69	-1,08	500
-1,08	-0,46	200

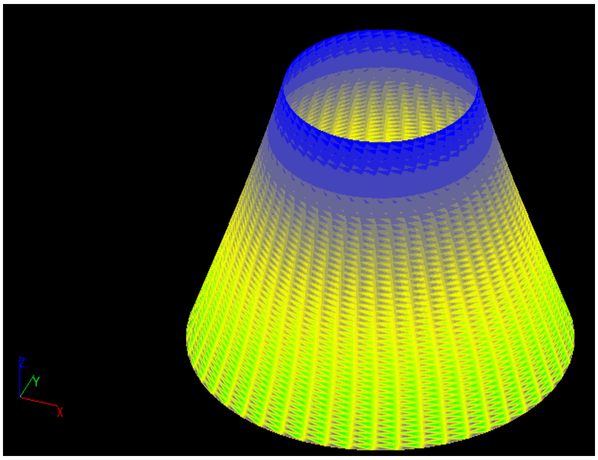

Figure 18. The Normal effort of Single-cavity hyperboloid of revolution about the y-axis

M_x		
кН*м/м	кН*м/м	
-0,6	-0,54	50
-0,54	-0,46	50
-0,46	-0,38	100
-0,38	-0,31	200
-0,31	-0,23	300
-0,23	-0,15	300
-0,15	-0,08	350
-0,08	0	3000
0	0,08	1700
0,08	0,15	1000
0,15	0,17	200

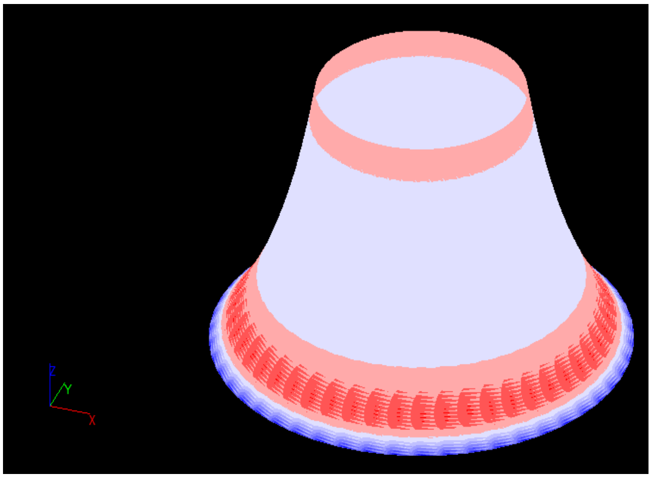

Figure 19. The bending Moment of Pseudosphere about the x-axis

M_x		
кН*м/м	кН*м/м	
-0,06	-0,06	50
-0,06	-0,05	50
-0,05	-0,04	100
-0,04	-0,04	100
-0,04	-0,03	150
-0,03	-0,02	200
-0,02	-0,01	250
-0,01	-0,01	200
-0,01	0	200
0	0,01	4550
0,01	0,01	600

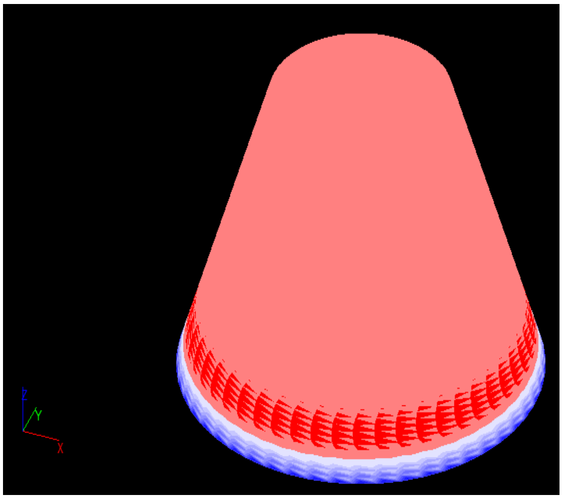

Figure 20. The bending Moment of Cone about the x-axis

M_x		
кН*м/м	кН*м/м	
-0,32	-0,29	50
-0,29	-0,25	50
-0,25	-0,21	150
-0,21	-0,17	200
-0,17	-0,12	200
-0,12	-0,08	300
-0,08	-0,04	300
-0,04	0	2950
0	0,04	1800
0,04	0,08	900
0,08	0,09	200

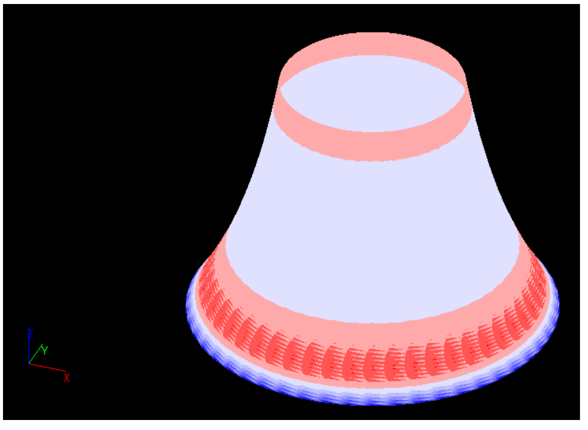

Figure 21. The bending Moment of Meridian – Hyperbole about the x-axis

M_x		
кН*м/м	кН*м/м	
-0,09	-0,09	50
-0,09	-0,08	50
-0,08	-0,06	100
-0,06	-0,05	100
-0,05	-0,04	150
-0,04	-0,03	200
-0,03	-0,02	250
-0,02	-0,01	200
-0,01	0	950
0	0,01	4000
0,01	0,02	700

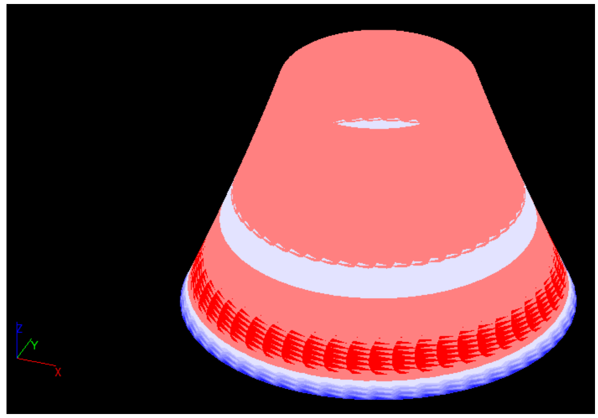

Figure 22. The bending Moment of Meridian – Asteroid about the y-axis

M_x		
кН*м/м	кН*м/м	
-0,01	-0,01	50
-0,01	-0,01	50
-0,01	-4,77e-003	100
-4,77e-003	-3,97e-003	100
-3,97e-003	-3,18e-003	150
-3,18e-003	-2,38e-003	200
-2,38e-003	-1,59e-003	250
-1,59e-003	-7,94e-004	200
-7,94e-004	0	200
0	7,94e-004	4500
7,94e-004	1,46e-003	700

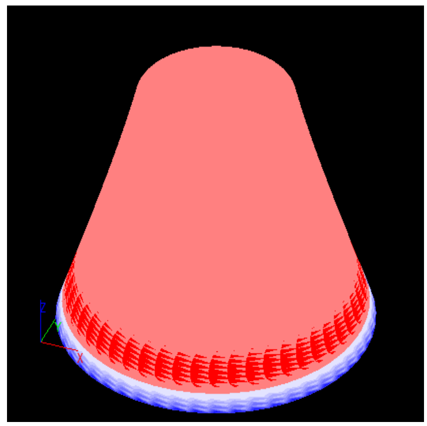

Figure 23. The bending Moment of Single-cavity hyperboloid of revolution about the x-axis

M_y		
кН*м/м	кН*м/м	
-0,59	-0,54	50
-0,54	-0,46	100
-0,46	-0,38	100
-0,38	-0,31	150
-0,31	-0,23	250
-0,23	-0,15	350
-0,15	-0,08	400
-0,08	0	2850
0	0,08	1900
0,08	0,15	950
0,15	0,18	300

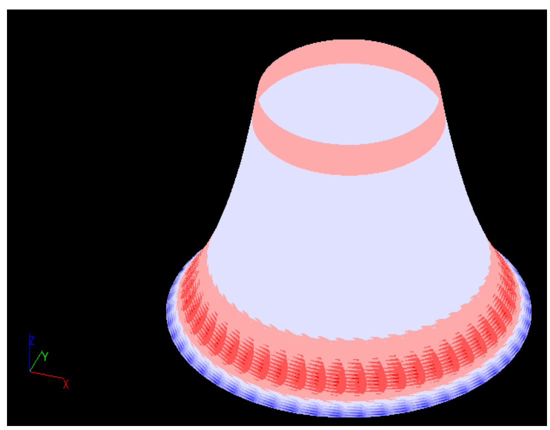

Figure 24. The bending Moment of Pseudosphere about the y-axis

M_y кН*м/м	кН*м/м	
-0,05	-0,05	50
-0,05	-0,05	50
-0,05	-0,04	50
-0,04	-0,03	50
-0,03	-0,03	200
-0,03	-0,02	200
-0,02	-0,01	250
-0,01	-0,01	200
-0,01	0	250
0	0,01	4550
0,01	0,01	600

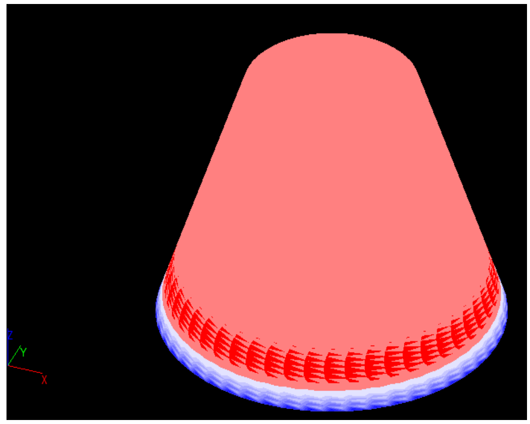

Figure 25. The bending Moment of Cone about the y-axis

кН*м/м	кН*м/м	
-0,32	-0,29	50
-0,29	-0,25	50
-0,25	-0,2	100
-0,2	-0,16	100
-0,16	-0,12	250
-0,12	-0,08	350
-0,08	-0,04	300
-0,04	0	3050
0	0,04	1850
0,04	0,08	950
0,08	0,09	250

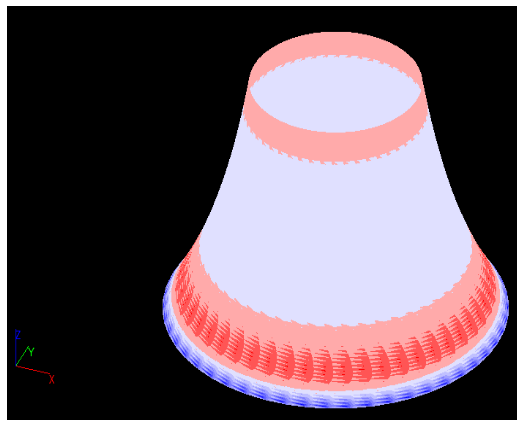

Figure 26. The bending Moment of Meridian – Hyperbole about the y-axis

M_y кН*м/м	кН*м/м	
-0,08	-0,08	50
-0,08	-0,07	50
-0,07	-0,06	50
-0,06	-0,05	50
-0,05	-0,04	200
-0,04	-0,03	200
-0,03	-0,02	250
-0,02	-0,01	300
-0,01	0	950
0	0,01	4100
0,01	0,02	700

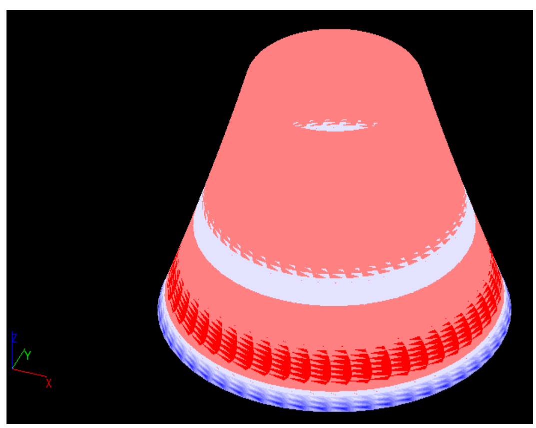

Figure 27. The bending-Moment of Meridian – Asteroid about the y-axis

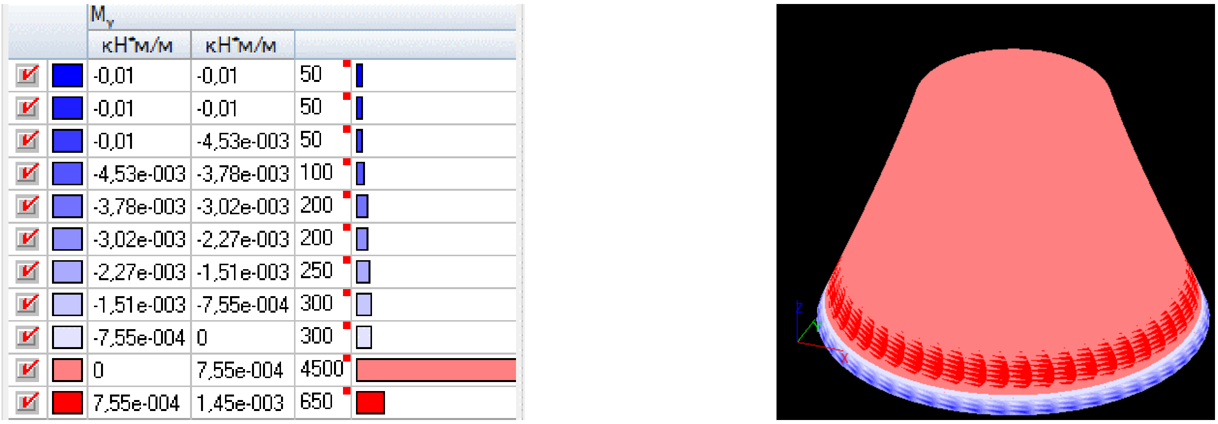

Figure 28. The bending-Moment of Single-cavity hyperboloid of revolution about the y-axis

4. Proposals for the use of pseudospherical shells in architecture and the construction industry

Figure 29. Stainless steel sculpture "Non Object", A. Kapoor, 2008

As noted earlier, no examples of the use of the surface of the pseudosphere in the construction industry have been found in the scientific and technical literature.

Only Kenneth Brecher [18] presented examples of pseudospheres implemented in nature: a gypsum model of the pseudosphere made by V.M. Schilling (V. Martin Schilling) at the end of the XIX century. The large-sized plywood pseudosphere model, Mathematica, exhibited at the Boston Science Museum, created by Charles and Ray Eames. Stainless steel sculpture for the park made by Anish Kapoor, 2008, fig. 26). The author — H. Sugimoto, 2004, made the model "The surface of revolution of constant negative curvature" and a sculpture made of aluminum and glass by the same author "Conceptual Form 009", 2006. Robert Le Ricolais make the "Funicular polygon of revolution — pseudosphere" metal wire shape. All these mathematical models serve educational purposes.

B. Bhattacharya [23] proposed to use a pseudo-spherical shell as the foundations of reinforced concrete chimneys. D. Werner [21] proposed to use a pseudo-spherical thin-walled shell as the base of the tower of the television station.

Basing his research on parametric equations of the pseudosphere, Zh. Kaydasov [31] introduced a new type of surfaces-multi-tube "pseudospheres" with external cycloidal and sinusoidal corrugations. In his opinion, these surfaces can attract the attention of architects. We take the name of the surface — "pseudosphere" — in quotes, because the proposed surface does not have a constant negative Gaussian curvature.

Additional information on the application of pseudospherical shells in building industry can be taken in a manuscript [33].

Conclusion

The areas of fragments of the considered surfaces of revolution with close geometric parameters are naturally compared with the minimum surface of revolution — the catenoid — the area of the fragment of which is determined by the formula:

$$A_{\text{кат}} = \pi\left[a^2 \ln\ \left|r + \sqrt{r^2 - a^2}\right| + r\sqrt{r^2 - a^2}\right]_{r2}^{r1},$$

where $a \le r_2$ – is the radius of the throat circumference lying in the *xOy*, plane, which is determined from the expression:

$$H = a\left(Arch\frac{r_1}{a} - Arch\frac{r_2}{a}\right). \quad (1)$$

The above two formulas must be used if the throat circumference of the catenoid is outside the considered fragment of the catenoid.

If the throat circumference is within the considered surface, as in our case, then these two formulas must be written in the following form:

$$A_{\text{кат}} = \pi\left[a^2 \ln\ \left|r + \sqrt{r^2 - a^2}\right| + r\sqrt{r^2 - a^2}\right]_{r2}^{a} + \\ + \pi\left[a^2 \ln\ \left|r + \sqrt{r^2 - a^2}\right| + r\sqrt{r^2 - a^2}\right]_{r1}^{a},$$

where $a \le r_2$ — the radius of the throat circle lying in the *xOy*, plane, which is defined from the expression:

$$H = a\left(Arch\frac{r_1}{a} + Arch\frac{r_2}{a}\right). \quad (2)$$

You can take the optimality factor over the area in the form:

$$\rho_{pow} = \frac{A_{pow}}{A_{cat.}} \ge 1.$$

Naturally, for the catenoid in this case $\rho_{pow} = 1$. However, for the case in question, $r_1 = 4$ m, $r_2 = 2$ m, $H = 5.15$ m the formulas (1), (2) have no solution, so compare the shells in question (Fig. 3) with a shell having a median minimum surface with the same geometric parameters, it is impossible. You can select the inverse task. First determine by the formula (2) $H_{max} = 3.65$m at $a = 1.448$ m for $r_1 = 4$ m, $r_2 = 2$ m, and then pick up the other shells of revolution.

We introduce the optimality factor over the area:

$$\rho_{\text{пов}} = \frac{A_{\text{пов}}}{A_{\text{псевд}}}.$$

The analyses showed that of the five shells presented in Fig. 3, the smallest area of the median surface has a shell with a hyperbola $z = b/x$ as a Meridian (ρ = 98.25/100.5 = 0.98). It is followed by a pseudosphere (ρ = 1), a shell with an asteroid (ρ = 102.86/100.5 = 1.02) as a Meridian, a unicellular hyperboloid of revolution (ρ = 103.1/100.5 = 1.03) and a cone (ρ = 104.1/100.5 = 1.04). The difference in surface areas shown in Fig. 3 is very small.

Comparing the isofields of efforts and displacements presented in Fig. 4—28, we can conclude that the pseudospherical shell has no particular advantages in this indicator either.

V.V. Novozhilov [29] wrote about the lack of demand for the catenoid, i.e. the only minimum surface rotation in construction in the near future. It will probably also be with a pseudospherical shell.

References

1. Trinker AB. High-rise building in extremal conditions. *Montazhnie i Spetz. Raboti v Stroitelstve*. 2017;9:15—19.
2. Esaulov GV. Modern problems and trends in architecture. *Zhilischnoe Stroitelstvo*. 2013;11:20—26.
3. Krivoshapko SN. *The History of Development of Architecture of Spatial Structures and Shells with Bases of Analysis*. Moscow: RUDN; 2015. (In Russ.)
4. Sysoeva EV. Scientific approaches to calculation and design of large-span structures. *Vestnik MGSU [Proceedings of Moscow State University of Civil Engineering]*. 2017;12,2(101):131—141. (In Russ.) http://dx.doi.org/10.22227/1997-0935.2017.2.131-141
5. Krivoshapko SN. On application of parabolic shells of revolution in civil engineering in 2000-2017. *Structural Mechanics of Engineering Constructions and Buildings*. 2017;4:4—14. (In Russ.) http://dx.doi.org/10.22363/1815-5235-2017-4-4-14
6. Grinko EA. Review papers on geometry, strength, stability, dynamics, and applications of shells with middle surfaces of diverse classes. *Montazhnie i Spetz. Raboti v Stroitelstve*. 2012;2:15—21. (In Russ.)
7. Mamieva IA, Razin AD. Symbol spatial structures in the form of conic surfaces. *Promyshlennoe i Grazhdanskoe Stroitelstvo*. 2017;10:5—11. (In Russ.)
8. Krivoshapko SN. The application of conoid and cylindroid in forming of buildings and structures of shell type. *Building and Reconstruction*. 2017;5(73):34—44.
9. Bandyopadhyay JN. *Thin Shell Structures: Classical and Modern Analysis*. New Age Int. Publ.; 1998.
10. Krivoshapko SN. Static, vibration, and buckling analyses and applications to one-sheet hyperboloidal shells of

revolution. *Applied Mechanics Reviews.* May 2002; 55(3):241—270.

11. Podgorniy AL, Grinko EA, Solovey NA. On research of new surface forms as applied to structures of diverse purpose. *RUDN Journal of Engineering Researches*, 2013;1:140—145. (In Russ.)

12. Popov AG. Pseudospherical surfaces and some problems of mathematical physics. *Fundamental and Applied Mathematics*. Izd. Dom "Otkrytie Sistemy" (MGU). 2005;11(1):227—239.

13. Brander D. Pseudospherical surfaces with singularities. *Annali di Matematica Pura ed Applicata.* June 2017;196(3):905—928.

14. Dorfmeister JF, Sterling I. Pseudo-spherical surfaces of low differentiability. *Advances in Geometry.* 2013;16(1):1—20. http://dx.doi.org/10.1515/advgeom-2015-0039

15. Coddington E. A Brief Account of the Historical Development of Pseudospherical Surfaces from 1827 to 1887... . Press of the New era printing Company, 1905, 74.

16. Kaydasov Zh. On three types of bobbin-shaped surfaces. *Dostizheniya Nauki i Obrasovaniya.* 2018;1(23):6-8.

17. Balazs NL, Voros A. Chaos on the pseudosphere. *Physics Reports.* 1986;143(3):109—240.

18. Brecher K. Mathematics, Art and Science of the. Pseudosphere. In: *Proceedings of Bridges 2013: Mathematics, Music, Art, Architecture, Culture. Netherlands, July 27-3, 2013.* Amsterdam; 2013. p. 469—472.

19. Ivanov VN, Krivoshapko SN. *Analytical Methods of Analysis of Shells of Non-Canonical Shape:* Monography. Moscow: RUDN; 2010.

20. Rekach VG. Momentless theory of analysis of pseudospherical shells. *Izv. Art. Inzh. Akademii*, 1958; 109.

21. Werner D. Ein Vergleich der Schnittkraftverteilung bei antimetrisch und symmtrisch belasteten Rotationsschalen. Wissenschaftliche Zeitschrift der Technischen Universität Dresden. 1967;16(4).

22. Krivoshapko SN. Drop-shaped, catenoidal, and pseudospherical shells. *Montazhnie i Spetz. Raboti v Stroitelstve*, 1998;11-12:28—32.

23. Bhattacharyya B. Shell-type foundation for R.C. Chimneys. *Indian J. Power and River Valley Develop.* 1982;32, 5-6:80—85.

24. Filin AP. On the theory of general sphere and pseudospherical shells. Stroit. *Mechanika i Raschet Sooruzheniy*, 1990;5:43—46. (In Russ.)

25. Mikheev AV. Local stability of pseudospherical orthotropic shells on the elastic base. *Izvestiya Sankt-Peterburgskogo Gos. Elektrotechnicheskogo Universiteta LETI.* 2013;7:9—15.

26. Jasion P, Magnucki K. *Buckling and post-buckling analysis of an untypical shells of revolution: Insights and Innovations in Structural Engineering, Mechanics and Computation. Proceedings of the 6th International Conference on Structural Engineering, Mechanics and Computation, SEMC 2016* 6th. 2016:766—771.

27. Jasion P, Magnucki K. *Theoretical investigation of the strength and stability of special pseudospherical shells under external pressure. Thin-Walled Structures.* 2015;93:88-93. http://dx.doi.org/10.1016/j.tws.2015.03.012

28. Krivoshapko SN, Emeliyanova YuV. To the question about the surface of revolution with geometrically optimal rise. *Montazhnie i Spetz. Raboti v Stroitelstve*. 2006;2:11—14. (In Russ.)

29. Novozhilov VV, Chernyh KF, Mikhailovskiy EI. *Lineynaya teoriya tonkih obolochek [Linear Theory of Thin Shells]*, Leningrad: Politehnika Publ.; 1991. (In Russ.)

30. Kalashnikov AA. Calculation of spatial thin-wall designs in the shape pseudospherical surface. *Structural Mechanics of Engineering Constructions and Buildings.* 2005;2:35—40. (In Russ.)

31. Kaydasov Zh. The pseudosphere with outer corrugations. *Academy*. 2018;3(30):3—5. (In Russ.)

32. Krawczyk J. Infinitesimal isometric deformations of a pseudo-spherical shell. *Journal of Mathematical Sciences*. 2002;109(1):1312—1320. (In Russ.)

33. Krivoshapko SN, Ivanov VN. Pseudospherical shells in building industry. *Building and Reconstruction*. 2018;2(76):32—40.

About the authors

Mathieu Gil-oulbé, Associate Professor of the Department of Civil Engineering, Academy of Engineering, RUDN University, Candidate of Technical Sciences; ORCID: 0000-0003-0057-3485; eLIBRARY ID: 27261171; e-mail: gil-oulbem@hotmail.com

Ipel Junior Alphonse Ndomilep, Graduate Student of the Department of Civil Engineering, Academy of Engineering, RUDN University; e-mail: ndomilepjunior@gmail.com

Prosper Ngandu, Master Student of the Department of Civil Engineering, Academy of Engineering, RUDN University; e-mail: prosperngandu60@gmail.com

Сведения об авторах

Жиль-улбе Матье, доцент департамента строительства инженерной академии РУДН, кандидат технических наук; ORCID: 0000-0003-0057-3485; eLIBRARY ID: 27261171; e-mail: gil-oulbem@hotmail.com

Ндомилеп Ипел Джуниор Альфонс, аспирант департамента строительства инженерной академии РУДН; e-mail: ndomilepjunior@gmail.com

Нганду Проспер, магистрант департамента строительства инженерной академии РУДН; e-mail: prosperngandu60@gmail.com